Structure and Electrochemical Studies of [(trispicMeen)ClFe^{III}OFe^{III}Cl(trispicMeen)]$^{2+}$. Spectroscopic Characterization of the Mixed-Valence Fe^{III}OFe^{II} Form. Relevance to the Active Site of Dinuclear Iron−Oxo Proteins

Alexander L. Nivorozhkin,[1a] Elodie Anxolabéhère-Mallart,[1a] Pierre Mialane,[1a] Roman Davydov,[1b] Jean Guilhem,[1c] Michèle Cesario,[1c] Jean-Paul Audière,[1a] Jean-Jacques Girerd,*[,1a] Stenbjorn Styring,*[,1b] Lutz Schussler,[1a] and Jean-Louis Seris[1d]

Laboratoire de Chimie Inorganique, URA CNRS 420, Institut de Chimie Moléculaire d'Orsay, Université Paris-Sud, 91405 Orsay, France, Institut de Chimie des Substances Naturelles, UPR CNRS 2301, 91198 Gif-sur-Yvette, France, Department of Biochemistry, Chemical Center, University of Lund, 22100 Lund, Sweden, and GRL, Groupe Elf Aquitaine, Lacq, 64170 Artix, France

Received August 18, 1995[⊗]

The dinuclear species [(trispicMeen)ClFe^{III}OFe^{III}Cl(trispicMeen)]Cl(OH)(H$_2$O)$_7$ (**1**) (trispicMeen = *N*,*N*,*N*′-tris-(2-pyridylmethyl)-*N*′-methylethane-1,2-diamine) was synthesized. It crystallizes in the monoclinic space group *C*2/*c* with $a = 33.87(2)$ Å, $b = 17.42(2)$ Å, $c = 23.41(5)$ Å, $\beta = 132.88(5)°$, $V = 10\,121(25)$ Å^3, and $Z = 8$. It contains an almost linear unit (Fe−O−Fe angle = 177.4(7)°). The potentially pentadentate ligand is in fact only tetracoordinated with one pyridine not bound to the metal ion. The octahedral coordination of Fe(III) is completed by one chloride ion. The structure of [(bispicMeen)ClFeOFeCl(bispicMeen)]Cl$_2$·CH$_3$COCH$_3$· 2H$_2$O (**2**) (bispicMeen = *N*,*N*′-bis(2-pyridylmethyl)-*N*′-methylethane-1,2-diamine) was also determined. It crystallizes in the monoclinic space group *C*2/*c* with $a = 11.124(4)$ Å, $b = 22.769(9)$ Å, $c = 15.874(6)$ Å, $\beta = 97.79(4)°$, $V = 3984(3)$ Å^3, and $Z = 4$. The main difference from **1** is that, in **2**, the Fe−O−Fe unit is bent with an FeOFe angle = 152.3(3)°. In cyclic voltammetry, **1** exhibits two reduction peaks at −0.230 and −0.960 V/SCE. They correspond respectively to the reduction to the Fe^{II}Fe^{III} and Fe^{II}Fe^{II} states. Cyclic voltammetry shows that the mixed-valent form [(trispicMeen)ClFe^{II}OFe^{III}Cl(trispicMeen)]$^+$ ($E° = -0.175$ V/SCE) is in equilibrium with another species ($E° = +0.065$ V/SCE) proposed to be [(trispicMeen)Fe^{II}OFe^{III}Cl(trispicMeen)]$^{2+}$ in which a chloride ion has been displaced by the originally unbound pyridine. The equilibrium constant was estimated to be 90 M^{-1}, and the rate of the recombination of chloride to the [(trispicMeen)Fe^{III}OFe^{III}Cl(trispicMeen)]$^{3+}$ complex was found equal to 3×10^5 M^{-1} s^{-1}. Controlled potential electrolysis of an acetonitrile solution of **1** allowed the preparation of the mixed-valent Fe(II)−O−Fe(III) form which gives an almost isotropic EPR signal similar to that already observed with oxo-bridged model compounds (Holz, et al. *Inorg. Chem.* **1993**, *32*, 5844. Hartman, et al. *J. Am. Chem. Soc.* **1987**, *109*, 7387) but different from the rhombic one observed in the mixed valent form of MMO. The mixed-valent forms slowly disproportionate to a mixture of Fe^{III}Fe^{III} and Fe(II) forms. The mixed-valent forms could be generated by radiolysis at 77 K, and an EPR study of the mixed-valent forms obtained by this procedure demonstrated that these species could not be protonated. Radiolysis of **1** at 77 K afforded the EPR spectrum of [(trispicMeen)ClFe^{II}OFe^{III}Cl(trispicMeen)]$^+$; upon annealing at 200 K, the solution gave an EPR spectrum very similar to that observed on the electrochemically reduced solution. This is in agreement with the observation of substitution of a chloride ligand. The mixed-valent form was not detected with the analogous complexes of the bispicen family: [(bispicMeen)ClFeOFeCl(bispicMeen)]Cl$_2$·CH$_3$COCH$_3$· 2H$_2$O (**2**) and [(bispicMe$_2$en)ClFeOFeCl(bispicMe$_2$en)]Cl$_2$ (**3**). Upon reduction, these complexes quickly (at CV time scale) decompose to mononuclear species.

Introduction

Exchange reactions of ligands in dinuclear iron−oxo complexes modeling the structural and functional properties of corresponding non-heme iron proteins have attracted much attention to aid in understanding the mechanism of catalytic activity.[2] However, there are only few reports on the reactivity involving terminal ligands.[3] The catalytic activity of the methane monooxygenase (MMO)[4] model complexes in oxidation reactions with hydrogen peroxide and organic peroxides has recently been shown to be strongly influenced by the nature of the terminal ligand.[5] The reaction mechanism implied involves transient peroxide adduct formed by ligand substitution. The problem of terminal ligand binding and exchange reactions was also considered with respect to the hemerythrin (Hr)[6] and

⊗ Abstract published in *Advance ACS Abstracts,* January 15, 1997.

(1) (a) Université Paris-Sud. (b) University of Lund. (c) Institut de Chimie des Substances Naturelles. (d) Groupe Elf Aquitaine.

(2) (a) Armstrong, W. H.; Spool, A.; Papaethymiou, G. S.; Frankel, R. B.; Lippard, S. J. *J. Am. Chem. Soc.* **1984**, *106*, 3653. (b) Armstrong, W. H.; Lippard, S. J. *J. Am. Chem. Soc.* **1985**, *107*, 3730. (c) Drüeke, S.; Wieghardt, K.; Nuber, B.; Weiss, J. *Inorg. Chem.* **1989**, *28*, 1414. (d) Drüeke, S.; Wieghardt, K.; Nuber, B.; Weiss, J.; Fleischauer, H.-P.; Gehring, S.; Haase, W. *J. Am. Chem. Soc.* **1989**, *111*, 8622. (e) Turowski, P. N.; Armstrong, W. H.; Roth, M. E.; Lippard, S. J. *J. Am. Chem. Soc.* **1990**, *112*, 681. (f) Bernard, E.; Moneta, W.; Laugier, J.; Chardon-Noblat, S.; Deronzier, A.; Tuchagues, J.-P.; Latour, J.-M. *Angew. Chem., Int. Ed. Engl.* **1994**, *33*, 887. (g) Hagen, K. S.; Lachicotte, R.; Kitaygorodskiy, A.; Elbouadili, A. *Angew. Chem., Int. Ed. Engl.* **1993**, *32*, 1321.

(3) (a) Mauerer, B.; Crane, J.; Schuler, J.; Wieghardt, K.; Nuber, B. *Angew. Chem., Int. Ed. Engl.* **1993**, *32*, 289. (b) Watton, S. P.; Masschelein, A.; Rebek, J., Jr.; Lippard, S. J. *J. Am. Chem. Soc.* **1994**, *116*, 5196. (c) Hazell, A.; Jensen, K. B.; McKenzie, C. J.; Toftlund, H. *Inorg. Chem.* **1994**, *33*, 3127.

S0020-1669(95)01084-6 CCC: $14.00

purple acid phosphatase[7] models. We report here the synthesis of a new dinuclear iron−oxo cation $[(trispicMeen)ClFe^{III}OFe^{III}Cl(trispicMeen)]^{2+}$ (trispicMeen = *N*,*N*,*N*′-tris(2-pyridylmethyl)-*N*′-methylethane-1,2-diamine) and its structure. The mixed-valence $Fe^{III}Fe^{II}$ form was characterized; in particular, an electrochemical study revealed ligand exchange in that half-reduced state. Fe(II) mononuclear complexes with the same ligand have been recently studied by Toftlund et al.[8]

Experimental Section

TrispicMeen. To a solution of *N*-methylethane-1,2-diamine (0.88 mL, 10 mmol) in acetonitrile (50 mL) containing KF/celite reagent (8 g)[9] was added picolyl chloride (30 mmol) in acetonitrile (20 mL), liberated by treating the corresponding hydrochloride (4.9 g, 30 mmol) with an equimolar amount of triethylamine. The reaction mixture was than heated with stirring for 2 h at 80 °C. After cooling, the solution was filtered and the filtrate evaporated to dryness in vacuo. The residual brown oil after column chromatography (neutral Al_2O_3, 50−200 mesh, eluent $CHCl_3$/EtOH 20:1) gave trispicMeen as a slightly yellow oil; yield, 1.75 g, 50%. ^{1}H NMR (250 MHz): δ 8.42−8.46 (m, 3H, *o*-py), 7.05−7.61 (m, 9H, H-py), 3.80 (s, 4H, 2CH_2-py), 3.59 (s, 2H, CH_2−py), 2.58−2.66 (m, 4H, 2CH_2−N), 2.15 (s, 3H, Me).

BispicMeen. This compound can be isolated as a minor fraction in the synthesis of trispicMeen or as a major product if the above reaction is carried out analogously using 20 mmol of the picolyl chloride; yield, 1.1 g, 47%. ^{1}H NMR (250 MHz): δ 8.41−8.49 (m, 2H, *o*-py), 7.08−7.74 (m, 6H, H−py), 3.86 (s, 2H, CH_2−py), 3.62 (s, 2H, CH_2−py), 2.57−2.68 (m, 4H, 2CH_2−N), 2.20 (s, 3H, Me).

bispicMe$_2$en.[10] This ligand was synthesized by alkylation of the *N*,*N*′-dimethylethane-1,2-diamine (10 mmol) with picolyl chloride (20 mmol) using a protocol similar to that for trispicMeen; yield, 2.45 g, 84%.

$[(trispicMeen)ClFeOFeCl(trispicMeen)]Cl(OH)(H_2O)_7$ (1), $[(bispicMeen)ClFeOFeCl(bispicMeen)]Cl_2\cdot CH_3COCH_3\cdot 2H_2O$ (2), and $[(bispicMe_2en)ClFeOFeCl(bispicMe_2en)]Cl_2$ (3). Addition to a solution of the corresponding ligand (1 mmol) in acetone (3 mL) of a solution of $[NEt_4]_2[Cl_3FeOFeCl_3]$ (0.5 mmol)[11] in acetone (3 mL) resulted in immediate formation of the precipitate which was filtered off and washed with acetone; yield, 70−80%.

$[(bispicMe_2en)FeCl_2]Cl$ (4) was obtained as an orange crystalline solid, by reaction of bispicMe$_2$en with $FeCl_3$ in acetone. Analyses were satisfactory.

Cyclic Voltammetry. Cyclic voltammetry was measured using an EGG 362 Princeton Inc. potentiostat and an *X*−*Y* chart recorder (SEFRAM). As the working electrode, glassy carbon (Tokai, Japan; Φ = 3 mm) was used. It was carefully polished with diamond pastes and ultrasonically rinsed in ethanol before each potential run. A Au wire was used as auxiliary electrode and a $Ag/AgClO_4$ electrode prepared in acetonitrile, separated by a fritted disk from the main solution as reference (300 mV above the potential of the saturated calomel electrode, SCE). The experiments were carried out in a double-wall Pyrex cell (thermostated at 25 °C) protected from light, on carefully degassed solutions by argon flushing.

Preparative Scale Electrolysis. They were carried out on a large glassy carbon electrode with the same reference electrode and a larger auxiliary electrode separated from the bulk solution by a large fritted disk. The charges were measured with a Tacussel IGN 5 integrator, and the intensity was measured with a Keithley 175 multimeter. The potential was imposed with an EGG 362potentiostat and controlled with a Keithley 175A multimeter.

UV−Vis Spectroelectrochemistry. The thin layer cell used for room temperature UV−vis experiments was previously described.[12] The working electrode was a platinum grid (0.3 mm). Reference and counter electrodes were the same as those used for cyclic voltammetry. Optical path of the cell was 0.5 mm.

Crystallographic Studies for 1. A crystal (0.025 × 0.25 × 1.1 mm^3) was mounted on a Philips PW 1100 diffractometer using graphite monochromated Mo Kα radiation. The main crystallographic data are given in Table 1. The structure was solved with SHELXS86 and refined with SHELX76. Surprisingly, a second chloride expected as counter-anion was not found in the crystal structure. The only hypothesis we can propose is the presence of an OH^- anion among the eight water molecules. The weighting scheme is $w = [\sigma^2(F) + 0.01F^2]^{-1}$. Refined atomic coordinates for significant atoms of the structure are given in Table 2.

Crystallographic Studies for 2. A crystal (0.15 × 0.3 × 0.9 mm^3) was mounted on a Philips PW 1100 diffractometer using graphite monochromated Mo Kα radiation. The main crystallographic data are given in Table 1. The structure was solved with SHELXS86 and refined with SHELX76. The weighting scheme is $w = [\sigma^2(F_o^2) + 0.015(F_o^2 + 2F_c^2)^2]^{-1}$. Refined atomic coordinates for significant atoms of the structure are given in Table 3.

Radiolytic Studies. For the radiolytic reduction solutions of complex **1** (≈2.5 mM) were made in dimethylformamide, dimethylformamide−water (1:1 by volume), and acetonitrile−acetone (1:2 by volume). The solutions or polycrystalline powder (≈30 mg) in quartz tubes (inner diameter 3.2 mm) were exposed to γ -rays from a ^{137}Cs source (dose rate 65 krad/h) for 30 h while immersed in liquid nitrogen. The irradiated solutions of **1** in acetone−acetonitrile and in dimethylformamide were annealed at 114 K for 30 s and at 144 K for 60 s, respectively, before EPR measurements, thereby decreasing the radical signals induced by solvent radiolysis by a factor of 30−100. The treatment induced no marked changes in the EPR signal from mixed-valent species. In order to follow the relaxation of the primary mixed-valent species trapped at 77 K, the samples were then annealed at higher temperatures (in isopentane for $T \geq 115$ K or *n*-pentane for $T > 144$ K) for suitable times followed by recooling to 77 K.

EPR spectra were recorded on a Bruker ESP 380E X-band EPR spectrometer using 100 kHz field modulation frequency, a liquid nitrogen cold finger dewar, or an Oxford Instrument ESR 9 liquid helium cryostat.

Table 1. Crystallographic Data for **1** and **2**

	1	**2**
formula	$C_{42}H_{65}Cl_3Fe_2N_{10}O_9$	$C_{33}H_{50}Cl_4Fe_2N_8O_4$
a, Å	33.87(2)	11.124(4)
b, Å	17.42(2)	22.769(9)
c, Å	23.41(5)	15.874(6)
β, deg	132.88(5)	97.79(4)
V, Å^3	10121(25)	3984(3)
Z	8	4
fw	1072.105	876.325
temp, K	293	293
space group	*C*2/*c*	*C*2/*c*
λ, Å	0.710 73	0.710 70
μ, mm^{-1}	0.79	1.043
R	6.4	7.4
R_w	8.2	10.4

(4) Abbrevations used in the article: MMO, methane monooxygenase; bispicen, *N*,*N*′-bis(2-pyridylmethyl)ethane-1,2-diamine; bispicMe$_2$en, *N*,*N*′-dimethyl-*N*,*N*′-bis(2-pyridylmethyl)ethane-1,2-diamine; bispicMeen, *N*-methyl-*N*,*N*′-bis(2-pyridylmethyl)ethane-1,2-diamine; trispicMeen, *N*,*N*,*N*′-tris(2-pyridylmethyl)-*N*′-methylethane-1,2-diamine; Benzimen, *N*′-(hydroxyethyl)-*N*,*N*,*N*′-tris(2-benzimidazolyl)ethane-1,2-diamine; t-tpchxn, *N*,*N*,*N*′,*N*′-tetra(2-pyridylmethyl)-*trans*-cyclohexane-1,2-diamine; TPA, tris(2-pyridylmethyl)amine.

(5) (a) Kojima, T.; Leising, R. A.; Yan, S.; Que, L., Jr. *J. Am. Chem. Soc.* **1993**, *115*, 11328. (b) Buchanan, R. M.; Chen, S.; Richardson, J. F.; Bressan, M.; Forti, L.; Morvillo, A.; Fish, R. H. *Inorg. Chem.* **1994**, *33*, 3208. (c) Menage, S.; Vincent, J. M.; Lambeaux, C.; Chottard, G.; Grand, A.; Fontecave, M. *Inorg. Chem.* **1993**, *32*, 4766.

(6) Beer, R. H.; Tolman, W. B.; Bott, S. G.; Lippard, S. J. *Inorg. Chem.* **1991**, *30*, 2082.

(7) Wilkinson, E. C.; Dong, Y.; Que, L., Jr. *J. Am. Chem. Soc.* **1994**, *116*, 8394.

(8) Bernal, I.; Jensen, I. M.; Jensen, K. B.; McKenzie, C. J.; Toftlund, H.; Tuchagues, J. P. *J. Chem. Soc., Dalton Trans.* **1995**, 3667−3675.

(9) Ando, T.; Yamawaki, J. *Chem. Lett.* **1979**, 45. Efficient application of the KF/Al_2O_3 reagent for the N-alkylation was also recently shown: Thangaraj, K.; Morgan, L. R. *Synth. Commun.* **1994**, *24*, 2063.

(10) Michelsen, K. *Acta Chem. Scand., Ser. A* **1977**, *31*, 429.

(11) Armstrong, W. H.; Lippard, S. J. *Inorg. Chem.* **1985**, *24*, 981.

(12) Lexa, D.; Savéant, J.-M.; Zickler, J. *J. Am. Chem. Soc.* **1977**, *99*, 2786.

Table 2. Fractional Coordinates for **1**

atom	*x*	*y*	*z*
O	2783(4)	21(5)	8806(5)
Fe1	2279(1)	734(1)	8114(1)
Cl1	2250(2)	1434(2)	8935(3)
CMe1	1580(7)	2242(8)	7109(10)
N11	1531(6)	1382(7)	7096(9)
C11	1103(6)	1210(8)	7110(10)
N111	1611(3)	18(5)	7678(5)
C211	1131(3)	346(5)	7286(5)
C311	690(3)	−38(5)	7060(5)
C411	738(3)	−797(5)	7240(5)
C511	1224(3)	−1148(5)	7640(5)
C611	1647(3)	−726(5)	7846(5)
C21	1370(7)	1070(9)	6366(11)
C31	1859(6)	985(8)	6485(9)
N21	2249(5)	447(6)	7151(7)
C41	2802(6)	602(8)	7474(9)
N121	2818(3)	1558(5)	8237(6)
C221	2999(3)	1375(5)	7893(6)
C321	3380(3)	1798(5)	7977(6)
C421	3589(3)	2442(5)	8436(6)
C521	3410(3)	2643(5)	8794(6)
C621	3029(3)	2191(5)	8682(6)
C51	2112(6)	−386(7)	6930(9)
N131	2732(5)	−942(6)	6854(6)
C231	2226(5)	−680(6)	6438(6)
C331	1824(5)	−704(6)	5626(6)
C431	1942(5)	−1010(6)	5211(6)
C531	2457(5)	−1282(6)	5622(6)
C631	2837(5)	−1238(6)	6434(6)
Fe2	3261(1)	−693(1)	9494(1)
Cl2	2895(2)	−1785(2)	8700(3)
CMe2	4204(7)	−1892(9)	10429(10)
N12	3883(6)	−1447(7)	10543(9)
C12	3584(7)	−1990(9)	10607(10)
N112	2907(4)	−990(5)	9957(5)
C212	3114(4)	−1595(5)	10442(5)
C312	2911(4)	−1870(5)	10751(5)
C412	2473(4)	−1514(5)	10558(5)
C512	2253(4)	−895(5)	10064(5)
C612	2479(4)	−652(5)	9778(5)
C22	4222(7)	−979(9)	11264(10)
C32	4350(7)	−215(9)	11100(10)
N22	3835(5)	173(6)	10444(7)
C42	3938(5)	725(6)	10066(7)
N122	3799(4)	−404(7)	9363(7)
C222	4032(4)	289(7)	9625(7)
C322	4325(4)	610(7)	9474(7)
C422	4385(4)	208(7)	9033(7)
C522	4151(4)	−501(7)	8759(7)
C622	3864(4)	−786(7)	8934(7)
C52	3562(7)	556(9)	10674(10)
N132	4223(5)	975(5)	12034(9)
C232	3882(5)	1201(5)	11287(9)
C332	3805(5)	1955(5)	11061(9)
C432	4088(5)	2511(5)	11622(9)
C532	4440(5)	2296(5)	12390(9)
C632	4495(5)	1530(5)	12571(9)

Results and Discussion

Structures of 1 and 2. The X-ray crystal structure of the complex dication $[(trispicMeen)ClFeOFeCl(trispicMeen)]^{2+}$ from **1** is represented in Figure 1. Selected distances are given in Table 4. The complex contains a Fe−O−Fe core with a corresponding angle of 177.4(7)°. This structure is reminiscent of that found[13] for $[(bispicen)ClFeOFeCl(bispicen)]^{2+}$ in which the Fe−O−Fe unit is linear by symmetry. In **1**, each iron atom is tetracoordinated to a trispicMeen ligand so that one of the pyridines of the $N(Picolyl)_2$ group is not coordinated.

(13) Arulsamy, N.; Hodgson, D. J.; Glerup, J. *Inorg. Chim. Acta* **1993**, *209*, 61.

Table 3. Fractional Coordinates for **2**

atom	*x*	*y*	*z*
Fe	403(1)	3660(1)	6470(1)
Cl1	−1199(1)	4241(1)	5849(1)
O	0	3470(2)	7500
N1A	2253(3)	3324(2)	6778(2)
N2A	1499(4)	4415(2)	6911(3)
C3A	1176(5)	4981(2)	6816(4)
C4A	1883(7)	5435(3)	7182(5)
C5A	2969(7)	5299(3)	7655(5)
C6A	3318(5)	4728(3)	7760(4)
C7A	2562(4)	4288(2)	7391(3)
C8A	2822(4)	3652(2)	7529(3)
C9A	2966(4)	3376(2)	6055(3)
N1B	1076(4)	3623(2)	5145(2)
N2B	−364(3)	2876(2)	5855(2)
C3B	−843(4)	2441(2)	6269(3)
C4B	−1366(5)	1954(2)	5876(4)
C5B	−1400(5)	1914(3)	4989(4)
C6B	−910(5)	2351(3)	4562(3)
C7B	−411(4)	2833(2)	4999(3)
C8B	93(5)	3343(2)	4577(3)
C9B	2161(5)	3231(2)	5248(3)
C10B	1368(6)	4200(2)	4793(4)

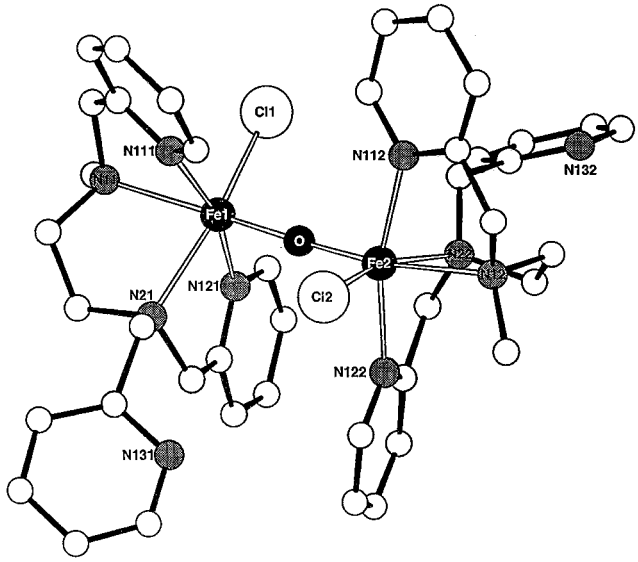

Figure 1. Crystal structure of the complex dication $[(trispicMeen)ClFe^{III}OFe^{III}Cl(trispicMeen)]^{2+}$ from **1**.

Table 4. Selected Bond Lengths (Å) and Angle (deg) for **1**

Fe1−O	1.822(10)	Fe2−O	1.792(10)
Fe1−Cl1	2.332(6)	Fe2−Cl2	2.341(4)
Fe1−N11	2.270(16)	Fe2−N12	2.270(15)
Fe1−N111	2.137(12)	Fe2−N112	2.155(15)
Fe1−N21	2.243(15)	Fe2−N22	2.261(12)
Fe1−N121	2.183(12)	Fe2−N122	2.106(18)
		Fe1−O−Fe2	177.4(7)

The structure of the complex cation $[(bispicMeen)ClFeOFeCl(bispicMeen)]^{2+}$ from **2** is represented in Figure 2. As compared to trispicMeen, the ligand bispicMeen lacks one picolyl arm. The cation $[(bispicMeen)ClFeOFeCl(bispicMeen)]^{2+}$ is very similar to that of **1** except for a notable reduction of the Fe−O−Fe angle to 152° (Table 5). A C_2 axis goes through the oxo bridging atom. The dramatic effect on the Fe−O−Fe angle of the nature of the substituents on the amino groups demonstrates the flexibility of the Fe−O−Fe unit. We note that a difference in the amino groups on one ligand seems to induce bending. On one hand, identical or very similar amino groups (NH,NH for $[(bispicen)ClFeOFeCl(bispicen)]^{2+}$ and NMe,-NCH_2py for **1**) lead to a linear Fe−O−Fe unit; on the other

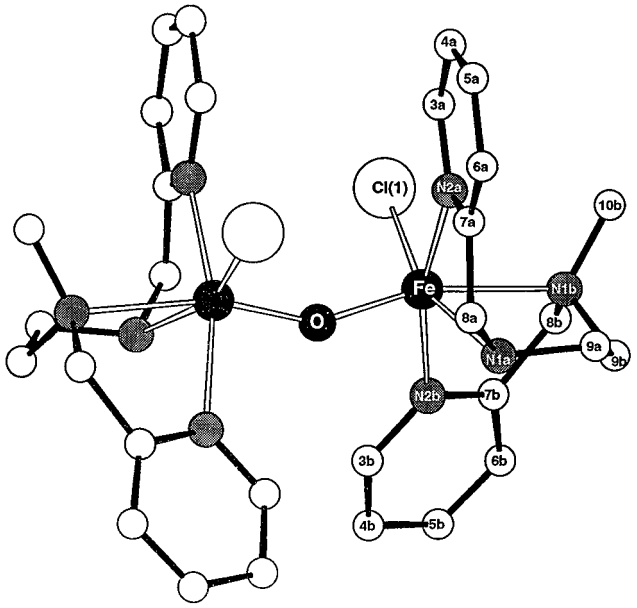

Figure 2. Crystal structure of the complex dication [(bispicMeen)-ClFe^{III}OFe^{III}Cl(bispicMeen)]$^{2+}$ from **2**.

Table 5. Selected Bond Lengths (Å) and Angle (deg) for **2**

Fe−O	1.8061(13)	Fe−N1a	2.187(4)
Fe−N2b	2.153(4)	Fe−N1b	2.327(4)
Fe−N2a	2.169(4)	Fe−Cl1	2.3277(14)
	Fe−O−Fe	152.3(3)	

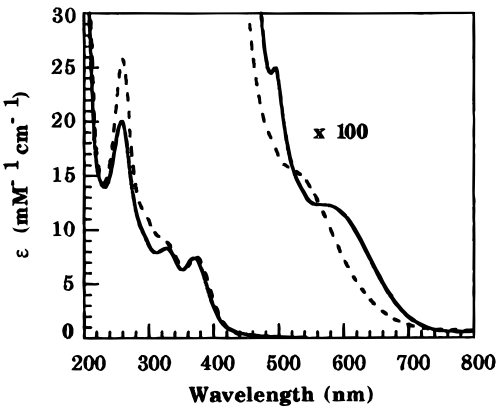

Figure 3. Comparison of the UV−vis spectra in acetonitrile of [(trispicMeen)ClFe^{III}OFe^{III}Cl(trispicMeen)]$^{2+}$ from **1** (- -) (linear Fe−O−Fe) and of [(bispicMeen)ClFe^{III}OFe^{III}Cl(bispicMeen)]$^{2+}$ from **2** (—)-(bent Fe−O−Fe).

hand, different amino groups (NH,NMe for **2**) lead to a bent Fe−O−Fe motif. One would thus predict that [(bispicMe$_2$en)-ClFeOFeCl(bispicMe$_2$en)]$^{2+}$ would have a linear Fe−O−Fe unit. This will be checked in the near future by X-ray diffraction. The linear versus bent geometry could be related to the better overlap of two pyridine groups, belonging to two different ligands, in **2** than in **1** or [(bispicen)ClFeOFeCl-(bispicen)]$^{2+}$, and thus to a stronger attraction between these groups. Comparing **1** and **2**, we note that in both cases the NMe group is trans to the O bridging group: the Fe−NMe distances are 2.270(15) and 2.327(4) Å respectively for **1** and **2**. The NCH$_2$py (**1**) or the NH (**2**) groups are trans to the Cl$^-$ ion with the following Fe−N distances equal to 2.261(12) and 2.187(4) Å respectively for **1** and **2**.

UV−Vis Spectroscopy of 1. The UV−vis spectrum of **1** in acetonitrile is represented in Figure 3. It presents absorption bands at 259 nm (ϵ = 28 000 M^{-1} cm^{-1}), 323 (10 000), 373 (8100), 522 (165), and 964 (8). It is quite similar to the spectrum of [(TPA)ClFeOFeCl(TPA)]$^{2+}$ as expected since the two systems have very similar structures.[14] The absorption is more intense in the UV and less intense in the visible than that of the bent [Fe$_2$O(RCO$_2$)$_2$] units,[15] as already pointed out by Que et al.[16]

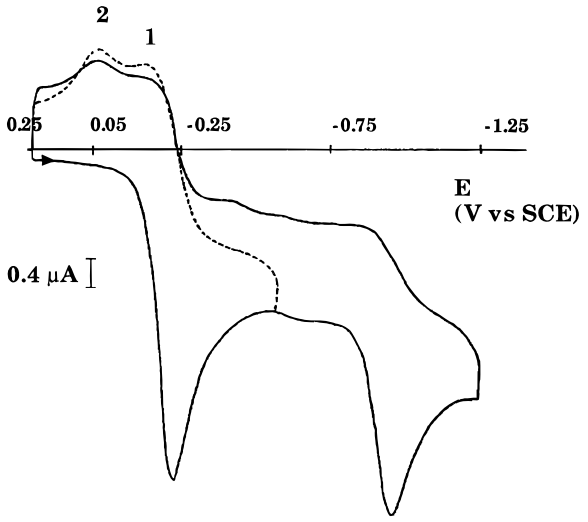

Figure 4. Cyclic voltammetry of **1** in acetonitrile in the presence of tetrabutylammonium perchlorate (0.1 M).

The influence of the Fe−O−Fe angle is illustrated by the spectra of **1** and **2** in Figure 3. Around 600 nm, the spectrum of **2** is more resolved and slightly more intense than that of **1**. This difference is clearly related to the value of the angle since, as pointed out above, the ligands are very close and the main difference is the bending of the Fe−O−Fe unit from **1** to **2**.

Redox Properties of 1. Redox properties of complexes with a (μ-oxo)diferric core are the subject of increasing attention.[16,17] These species reveal two consecutive one-electron reduction processes, affording Fe^{II}Fe^{III} and Fe^{II}Fe^{II} species, the latter process being rarely reversible. Cyclic voltammetry of an acetonitrile solution of **1**, using tetrabutylammonium perchlorate as supporting electrolyte and obtained with a scan rate of 100 mV s^{-1}, is shown in Figure 4. Two reduction peaks are observed at −0.230 and −0.960 V/SCE, corresponding to the successive formation of the Fe^{II}Fe^{III} and Fe^{II}Fe^{II} species, respectively. We concentrated our study on the first reduction. In these conditions, two reoxidation peaks are obtained at −0.15 (peak 1) and +0.030 V (peak 2).

The origin of the two oxidation peaks was studied. Figure 5(top) shows changes in the voltammograms upon increasing concentration of the chloride ions. Addition of tetrabutylammonium chloride does not influence the cathodic wave. However, anodic wave 2 vanishes, whereas wave 1 increases in intensity. Addition of silver perchlorate leads to the opposite effect, *i.e.*, to an increase of the intensity of wave 2 accompanied by a decrease of wave 1 (not shown). Variation of the cyclic voltammograms with a change in scan rate was also studied (Figure 5(bottom)). The cathodic wave at −0.23 V remains diffusion controlled upon varying the scan rate from 50 to 200 mV s^{-1}, but for the reverse scan we observed an enhancement of anodic wave 2 relative to wave 1. This behavior can be

(14) Norman, R. E.; Holz, R. C.; Ménage, S.; O'Connor, C. J.; Zhang, J. H.; Que, L., Jr. *Inorg. Chem.* **1990**, *29*, 4629−4637.
(15) Bossek, U.; Hummel, H.; Weyhermüller, T.; Bill, E.; Wieghardt, K. *Angew. Chem., Int. Ed. Engl.* **1995**, *34*, 2642−2645.
(16) Holz, R. C.; Elgren, T. E.; Pearce, L. L.; Zhang, J. H.; O'Connor, C. J.; Que, L., Jr. *Inorg. Chem.* **1993**, *32*, 5844.
(17) Hartman, J. R.; Rardin, R. L.; Chaudhuri, P.; Pohl, K.; Wieghardt, K.; Nuber, R.; Weiss, J.; Papaefthymiou, G. C.; Frankel, R. B.; Lippard, S. J. *J. Am. Chem. Soc.* **1987**, *109*, 7387.

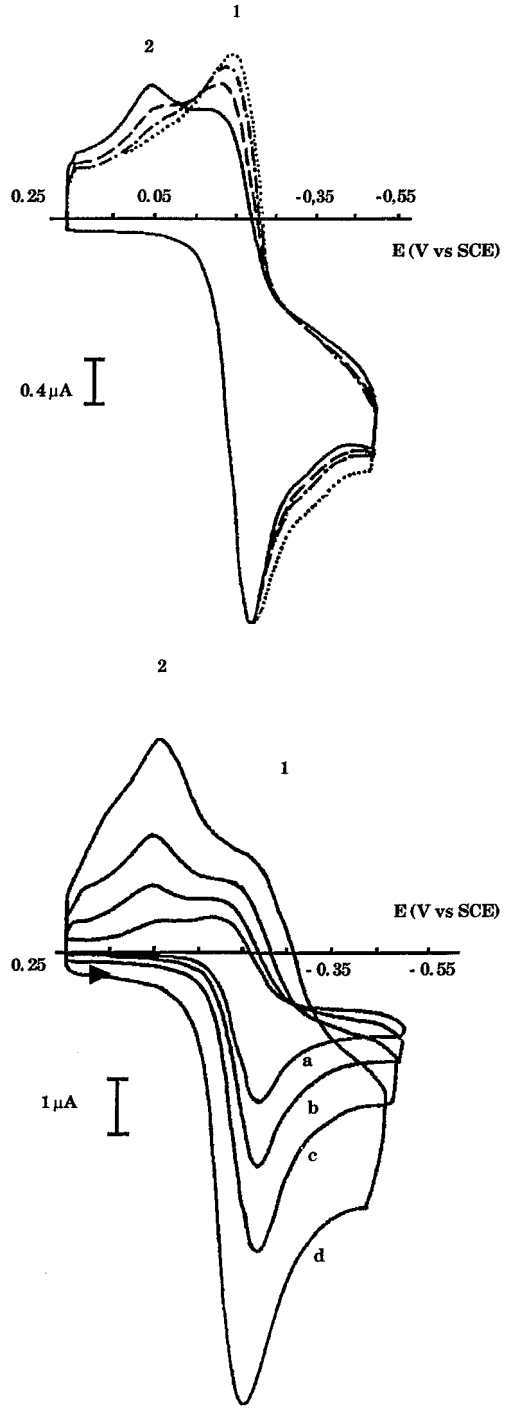

Figure 5. Cyclic voltammetry of **1** in acetonitrile in the presence of tetrabutylammonium perchlorate (0.1 M) (top) Influence of the chloride concentration (- -) $[Cl^-] = 0.6$ mM; (− · −) $[Cl^-] = 1.2$ mM; (···) $[Cl^-] = 2$ mM. (bottom) Influence of the scan rate: (a) 50, (b) 100, (c) 200 and (d) 500 mV s^{-1}.

rationalized by the following reaction sequence (Scheme 1). The reduction of the $[LClFe^{III}OFe^{III}ClL]^{2+}$ (L stands for trispicMeen) complex generates the mixed-valent complex $[LClFe^{II}OFe^{III}ClL]^{+}$ which exists in equilibrium with the monochloro $[LFe^{II}OFe^{III}ClL]^{2+}$ species formed by dissociation of one of the terminal chloride ligands. Upon reoxidation, these mixed-valent species show two different potentials. The monochloro $[LFe^{II}OFe^{III}ClL]^{2+}$ species is reoxidized at more positive potential (peak 2) than the dichloro $[LClFe^{II}OFe^{III}ClL]^{+}$ complex (peak 1). In order to observe a cathodic wave corresponding to the reduction of the monochlorodiferric species $[LFe^{III}OFe^{III}ClL]^{3+}$, we first generated the two mixed-valent species within the

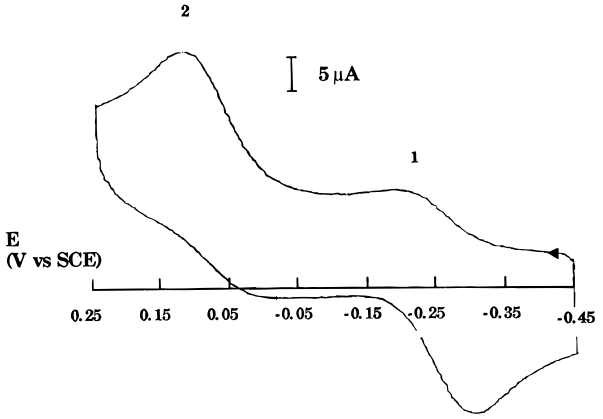

Figure 6. Cyclic voltammetry (scan rate 200 V s^{-1}) of **1** in acetonitrile in the presence of tetrabutylammonium perchlorate (0.1 M) with glassy carbon working electrode from −0.45 V to +0.25 V vs SCE.

Scheme 1

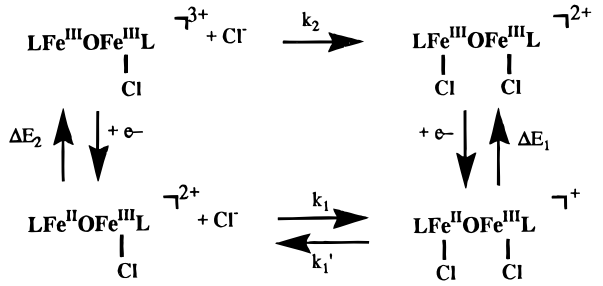

diffusion layer by setting the electrode potential at −0.450 V. Cycling then the potential between this value and +0.250 V at a scan rate of 200 V s^{-1} allowed us to detect a cathodic peak at +0.015 V attributed to the reduction of $[LFe^{III}OFe^{III}ClL]^{3+}$ to $[LFe^{II}OFe^{III}ClL]^{3+}$ (Figure 6). The fact that this peak was not observed at lower scan rates is due to the very rapid complexation of chloride ions by $[LFe^{III}OFe^{III}ClL]^{3+}$. The rate constant k_2 of this process can be estimated to be of the order of 3×10^5 M^{-1} s^{-1}. This value can be compared to that ($>9 \times 10^7$ M^{-1} s^{-1}) in the case of an iron(III) tetraphenylporphyrin.[18] From the fast-scan experiment we can also estimate an equilibrium constant for interconversion between the mixed-valent species. At such high rates, the system attained a frozen equilibrium situation, allowing the determination of the concentration ratio of the two mixed valent forms from the ratio of the peak intensities and thus the equilibrium constant which was found equal to $K_1 = k_1/k_1' = 90$ M^{-1}. This value is in agreement with that measured (56 M^{-1}) for iron(II) tetraphenylporphyrin.[18] Moreover, this experiment gave the value $E° = +0.065$ V/SCE for the $[LFe^{III}OFe^{III}ClL]^{3+}/[LFe^{II}OFe^{III}ClL]^{3+}$ couple. The experiment at high chloride concentration gave $E° = -0.175$ V/SCE for the $[LClFe^{III}OFe^{III}ClL]^{2+}/[LClFe^{II}OFe^{III}ClL]^{2+}$ couple. From these values, one can deduce $K_2 = K_1 \times 10^4 = 9 \times 10^5$ M^{-1}. Again, this value is in agreement with that measured (2×10^5 M^{-1}) for iron(III) tetraphenylporphyrin.[18]

The nature of the group substituting the chloride ion is not known. One attractive hypothesis is that this equilibrium is a result of a ligand-induced transformation where the Fe(II) ion becomes fully coordinated by the pentadentate trispicMeen because of the larger ionic radius for Fe(II). Therefore, for Fe(II) there would be an efficient competition between chloride and pyridine ligands. In fact Toftlund et al. have isolated

(18) Lexa, D.; Rentien, P.; Savéant, J.-M.; Xu, F. *J. Electroanal. Chem.* **1985**, *191*, 253−279.

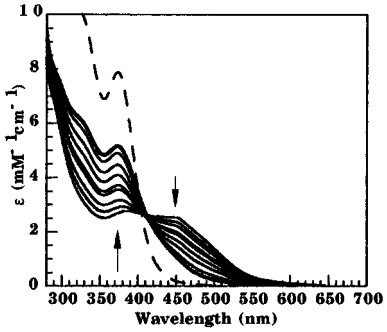

Figure 7. UV−vis spectroelectrochemistry as a function of time of the electrochemically reduced acetonitrile solution of [(trispicMeen)-ClFe^{III}OFe^{III}Cl(trispicMeen)]$^{2+}$ kept under argon; tetrabutylammonium perchlorate (0.1 M): (- -) Starting Fe^{III}Fe^{III} form with no applied potential; (—) $E = -0.45$ V vs SCE Fe^{III}Fe^{II}. The arrows show the evolution of the mixed-valent form under argon with no applied potential.

mononuclear [Fe(II)(trispicMeen)X]$^+$ (X = Cl, NCS, CN) complexes.[8] We have also showed by X-ray crystallography that the Fe(II) is completely coordinated by trispicMeen in [Fe^{II}-(trispicMeen)Cl]$^+$.[19]

Spectroscopic Characterization of the Fe^{II}Fe^{III} Form. Electrochemical Preparation. Controlled potential electrolysis of an acetonitrile solution of **1** was performed at −0.450 V. Coulommetry indicates one-electron reduction of the Fe^{III}Fe^{III} unit**.** The UV−visible spectrum, obtained by spectroelectrochemistry, of the mixed-valent form is represented in Figure 7. It presents absorption bands at 383 nm (3000 $M^{-1}cm^{-1}$) and 452 (2740). These are much more intense than those of the [(MeTACN)$_2$Fe$_2$(OH)(RCO$_2$)$_2$]$^{2+}$ reported by Wieghardt et al.[15] To our knowledge there has been no Fe(II)−O−Fe(III) characterized by UV−vis spectroscopy.

A sample was taken from the electrolyzed solution of **1** and immediately frozen at 77 K. It displays at 4.2 K a slightly axial EPR signal with $g_\perp = 1.96$ and $g_\parallel \approx 1.92$ (shoulder), characteristic of an antiferromagnetically coupled Fe^{II}(high spin)Fe^{III}-(high spin) system (Figure 8). This signal is closer to that observed in model compounds with an oxo bridge[16,17] than to the rhombic one observed in MMO[20,21] or for the model complex [(MeTACN)$_2$Fe$_2$(OH)(RCO$_2$)$_2$]$^{2+}$ [15] which have an OH bridging group. From our CV study, it is clear that this solution contains a mixture of both [LClFe^{III}OFe^{II}ClL]$^+$ and [LClFe^{III}OFe^{II}L]$^{2+}$ mixed-valent forms.

Wieghardt[15] recently demonstrated that the mixed-valent complex [(MeTACN)$_2$Fe$_2$(OH)(RCO$_2$)$_2$]$^{2+}$ slowly disproportionates to a Fe^{II}Fe^{II} and Fe^{III}Fe^{III} mixture. We suspected that the same phenomenon occurred here. Indeed, the UV−visible spectrum of a solution of the mixed-valent form kept under argon with no applied potential[22] slowly (1 h) changed, as

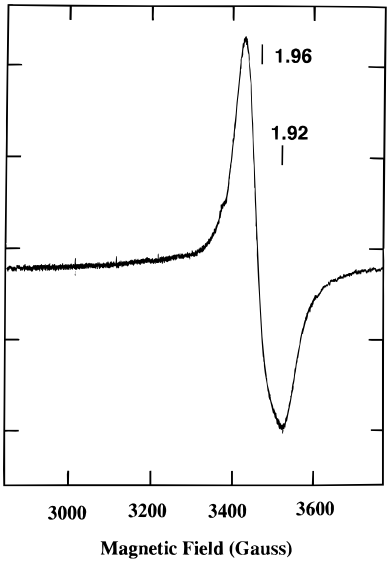

Figure 8. EPR spectrum of an electrochemically reduced acetonitrile solution of [(trispicMeen)ClFe^{III}OFe^{III}Cl(trispicMeen)]$^{2+}$. Spectrometer settings: modulation frequency, 100 kHz; modulation amlpitude, 5 G; receiver gain, 5×10^3, microwave power, 1 mW; 4.2 K; $\nu = 9.428$ GHz.

represented in Figure 7. We do not know the spectrum of the Fe^{II}Fe^{II} form(s) involved which prohibits a detailed analysis of the resultant spectrum, although the appearance of some features of the Fe^{III}Fe^{III} spectrum is clear. Correspondingly the EPR spectrum disappears. We do not know the fate of the dinuclear Fe(II) species. One possibility is that it transforms into mononuclear [(trispicMeen)Fe^{II}X]$^{n+}$ species which are known to exist.[8,19]

Radiolytic Study. Along with standard electrochemical reduction we have also generated the mixed-valent state of complex **1** by one-electron reduction of the diferric unit in solid solutions or polycrystalline powder at 77 K by mobile electrons generated by γ-irradiation.[23−26] This technique was earlier successfully applied for the generation and EPR study of kinetically stabilized mixed-valent states in dinuclear iron−oxo sites in proteins[23,24,26,27] or in various model compounds.[24,27] At 77 K, molecular dynamics is limited and the primary mixed-valent product by this cryogenic reduction most likely retains a ligand environment similar to that of the initial diferric state. Therefore the conformation of this primary mixed-valent species is expected to be in a constrained, non-equilibrium state, if the structure of the coordination sphere depends on the oxidation level of the iron ions. Thus, the reduction at 77 K may be regarded as producing an EPR probe for structural studies of the original Fe^{III}Fe^{III} dinuclear iron site, which itself is EPR silent. At higher temperatures this constrained, non-equilibrium ligand environment relaxes to the corresponding equilibrium state.

EPR spectra of the primary mixed-valent species produced by radiolytic reduction at 77 K of complex **1** in acetone−acetonitrile and dimethylformamide glass as well as in polycrystalline powder, are presented in Figure 9. The cryogenically

(19) Mialane, P.; Guilhem, J.; Girerd, J.-J. unpublished results.
(20) In MMO, the signal of the mixed valence-form is rhombic with $g_z = 1.94$, $g_y = 1.86$, $g_x = 1.75$. See: Fox, B. G.; Surerus,K. K.; Münck, E.; Lipscomb, J. D. *J. Biol. Chem.* **1988**, *263*, 10553−10556. DeWitt, J. G.; Bentsen, J. G.; Rosenweig, A. C.; Hedman, B.; Green, J.; Pilkington, S.; Papaefthymiou, G. C.; Dalton, H.; Hodgson, K. O.; Lippard, S. J. *J. Am. Chem. Soc.* **1991**, *113*, 9219−9235. See also: Fox, B. G.; Hendrich, M. P.; Surerus, K. K.; Anderson, K. K.; Froland, W. A.; Lipscomb, J. D.; Münck, E. *J. Am. Chem. Soc.* **1993**, *115*, 3688−3701. In MMO, the mixed-valent pair contains an hydroxo bridge as proven by: Thomann, H.; Bernardo, M.; McCormick, J. M.; Pulver, S.; Anderson, K. K.; Lipscomb, J. D.; Solomon, E. I. *J. Am. Chem. Soc.* **1993**, *115*, 8881−8882.
(21) De Rose, V. J.; Liu, K. E.; Kurtz, D. M., Jr.; Hoffman, B. M.; Lippard, S. J. *J. Am. Chem. Soc.* **1993**, *115*, 6440−6441.
(22) If the potential is kept for a long time at −0.45 V/SCE, a solution containing Fe(II) is obtained by further reduction of the Fe^{III}Fe^{III} species.
(23) Davydov, R.; Kuprin, S.; Gräslund, A.; Ehrenberg, A. *J. Am. Chem. Soc.* **1994**, *116*, 11120−11128.
(24) Davydov, R.; Sahlin, M.; Kuprin, S.; Gräslund, A.; Ehrenberg, A. *Biochemistry* **1996**, *35*, 5571−5576.
(25) Davydov, R.; Ménage, S.; Fontecave, M.; Gräslund, A.; Ehrenberg, A. *J. Biol. Inorg. Chem.*, in press.
(26) Blumenfeld, L.; Burbaev, D.; Davydov, R. In *The Fluctuating Enzyme*; Welch, G. R., Ed.; Wiley: New York, 1986; pp 369−401.
(27) Davydov, R.; Gräslund, A.; Ehrenberg, A.; Bowman, M.; Smieja, J.; Dikanov, S. *J. Inorg. Biochem.* **1995**, *59*, 395

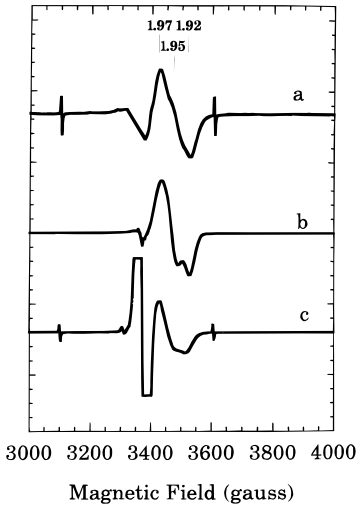

Figure 9. EPR spectra of the primary mixed-valent forms of complex **1** in the polycrystalline powder (a) as well as in dimethylformamide (b) and dimethylformamide−water (1:1) (c) glasses produced by radiolytic reduction at 77 K. The intense resonance centered at $g = 2.00$ arises from trapped free radicals induced by the γ-radiolysis. A pair of sharp lines centered at $g = 2.00$ and split by 50.5 mT are due to trapped hydrogen atoms (peak at about 3620 G). Spectrometer settings are the same as those in Figure 8 except for the temperature, 77 K; the microwave power, 9.2 mW; and the microwave frequency, 9.462 GHz.

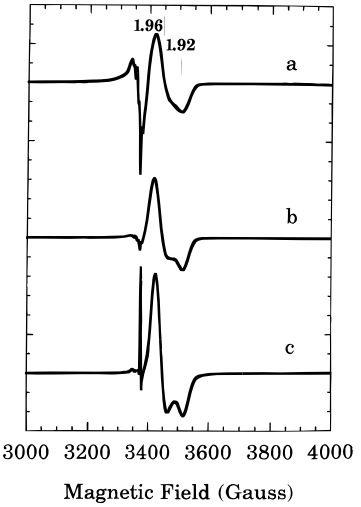

Figure 10. EPR spectra at 77 K of the mixed-valent form of complex **1** in acetonitrile−acetone (a), dimethylformamide (b), and dimethylformamide−water (1:1) glasses (c) produced after annealing at 195 K for 40 s (a), 240 K for 60 s (b), and 220 K for 30 s (c). The mixed-valent state was generated by radiolytical reduction at 77 K. EPR settings as in Figure 9.

reduced complex in the powder sample displays a poorly resolved, rhombic EPR signal, Figure 9a, with a narrow spread in g-values ($g_1 = 1.974$, $g_2 = 1.945$, and $g_3 = 1.917$). The EPR spectrum of the mixed-valent form of **1** produced at 77 K in dimethylformamide is characterized by effective g-values of 1.968, 1.948, and 1.915 (Figure 9b). Complex **1** reduced at 77 K in acetone−acetonitrile glass gives rise to an identical mixed-valent signal (not shown). In contrast, the primary mixed-valent species trapped at 77 K in a water−dimethylformamide (1:1) glass gives an axial EPR spectrum (Figure 9c) with $g_\perp = 1.956$ and $g_\parallel = 1.924$,which is very close to that for **1** reduced electrochemically. All of these mixed-valent EPR signals are observable without notable broadening up to about 100 K. EPR signals with low g-anisotropy ($g_{av} \approx 1.92-1.95$; $\Delta g \leq 0.06$) and long T_1 have previously been shown to be characteristic of oxo-bridged mixed-valent diiron clusters with antiferromagnetically coupled Fe(II)(S=2) and Fe(III)(S=$^5/_2$) ions.[24,27]

The mixed-valent forms of complex **1** that are generated either by electrochemical means in acetonitrile at room temperature or by low temperature reduction at 77 K produce slightly different EPR spectra (cf. spectra of Figures 8 and 9b). Normally the EPR properties of $Fe^{II}Fe^{III}$ clusters are mainly determined by the structure of the coordination sphere of the Fe(II) ion.[28,29] Therefore the spectral distinctions provide evidence that the ligand environment of Fe(II) in these mixed-valent species is different. Furthermore, our observation that the complex in the mixed-valent state trapped at 77 K in solid solutions (acetone−acetonitrile, dimethylformamide) or in the powder form display slightly distinct EPR spectra (cf. Figure 9, traces a and b) implies that the complex in solution and in solid state has slightly different configurations. Presently we cannot identify these differences, and additional information is needed to understand the structural distinctions in detail.

During annealing at temperatures above 195 K, constrained, non-equilibrium configurations of the primary mixed-valent species trapped at 77 K in solid solutions relax toward their equilibrium state. Progressive annealing of the sample of the cryogenically reduced complex **1** in acetone−acetonitrile at 195 K for 45 s resulted in the appearance of a new axial signal with $g_\perp = 1.96$ and $g_\parallel = 1.926$ (Figure 10a) identical to that of **1** in the mixed-valent state generated at room temperature (Figure 8). In contrast, the relaxed mixed-valent forms of complex **1** in dimethylformamide and in the water−dimethylformamide mixture (produced by annealing of the sample irradiated at low temperature at 240 K for 60 s) give rise to axial EPR signals with $g_\perp = 1.96$ and $g_\parallel \approx 1.92$ (Figure 10b,c) which slightly differ in shape from the spectrum in Figure10a. These distinctions are likely due to the influence of solvents on the configuration of **1** in the mixed-valent state. It is worth noting that the annealing at 240 K for 60 s of the powder sample irradiated at 77 K does not influence the mixed-valent signal shape and results only in decreasing the amplitude of the mixed-valent signal by 70%.

These results are in good agreement with the observation of two forms of the mixed-valent complex **1**, $[LClFe^{II}OFe^{III}ClL]^+$ and $[LFe^{II}OFe^{III}ClL]^{2+}$ (Scheme 1). Reduction at 77 K of the complex cation of **1**, $[LClFe^{III}OFe^{III}ClL]^{2+}$, in frozen solutions or in the solid state results in the formation of the kinetically stabilized mixed-valent dichloro $[LClFe^{II}OFe^{III}ClL]^+$ species, which give rise to characteristic EPR signals (Figure 9a,b). Upon progressive annealing at temperatures above 195 K in solution this mixed-valent species is transformed into the equilibrium mixture of $[LClFe^{II}OFe^{III}ClL]^+$ and $[LFe^{II}OFe^{III}ClL]^{2+}$ with the $S = {}^1/_2$ EPR spectra shown in Figure 10a,b. In the powder sample this transition is sterically hindered because of the rigid environment. Thus, there is no change of the EPR spectrum upon annealing of the irradiated sample at high temperatures. In aqueous solution complex **1** is expected to be dissociated into $[LFe^{III}OFe^{III}ClL]^{3+}$ (or possibly $[LFe^{III}OFe^{III}L]^{4+}$) and Cl^-. Upon cryogenic reduction the $[LFe^{III}OFe^{III}ClL]^{3+}$ species will form $[LFe^{II}OFe^{III}ClL]^{2+}$ as the primary product. However, the EPR spectra of the relaxed mixed-valent species are different in the different solvents (Figure 10). This suggests that the conformation of the mixed-valent species is affected by the environment.

As said before, the characteristics of the EPR signal (weak anisotropy and long T_1) demonstrate that the oxo bridge in the

(28) Sands, R. H.; Dunham, W. R. *Q. Rev. Biophys.* **1975**, *7*, 443−504.
(29) Bertrand, P.; Guigliareli, B.; More, C. *New J. Chem.* **1991**, *15*, 445−454.

mixed-valent state of complex **1** is not protonated in aqueous solution. This is in contrast to the majority of oxo bridges in $Fe^{II}OFe^{III}$ centers in various proteins and model compounds, which, when they are produced by radiolytic reduction at 77 K, become protonated upon annealing at higher temperatures.[23−25,27] This implies that the terminal ligand in the complex can exert a strong effect on the p*K* of the oxo−ligand in mixed-valent binuclear iron centers.

Comparison with Systems using bispicen-Type Ligands. We decided to reexamine the redox chemistry of some bispicen-type complexes assuming that these would be good models for assessing the role of ligand modifications. We studied, by cyclic voltammetry, the complex [(bispicMeen)ClFeOFeCl(bispicMeen)]Cl_2 (**2**) and [(bispicMe_2en)ClFeOFeCl(bispicMe_2en)]Cl_2 (**3**).[30]

The redox behavior of the bispicen-type complexes was reported[13] as irreversible with a single cathodic wave not specified but lying in the range from −0.56 to −0.76 V vs SCE. We also found a similar irreversible $Fe^{III}Fe^{III}/Fe^{II}Fe^{III}$ reduction at −0.430 V for **2**, which, however, was accompanied by an anodic peak at 0.125 V. The second and subsequent repetitive scans resulted in occurrence of a new reduction peak at 0.055 V. We assigned these new peaks to the same reversible redox couple with $E_{1/2} = 0.090$ V. Similar transformations were detected for **3**, where a new redox couple appears at more positive potential, $E_{1/2} = 0.165$ V. This behavior suggests that the mixed-valent species generated from **2** and **3** readily decompose to a mixture of $[L'ClFe^{III}OFe^{III}ClL']^{2+}$ and of the mononuclear complex $L'Fe^{II}Cl_2$. This was checked with [(bispicMe_2en)$FeCl_2$]Cl[31] (**4**), which demonstrated a reversible Fe^{III}/Fe^{II} reduction at $E_{1/2} = 0.165$ V, very similar to that found for **2** and **3**.

Conclusion

From this study, we can conclude that incorporation of the complementary ligand pyridyl arm in complex **1** plays a significant role in stabilizing kinetically the mixed-valent form as compared to the tetradentate ligands of the bispicen type. One reason could be that the hanging extra pyridine arm hinders the approach of two $Fe^{II}Fe^{III}$ units and thus makes the disproportionation reaction to $Fe^{III}Fe^{III}$ and $Fe^{II}Fe^{II}$ much slower for **1** than for the bispicen-type complexes. This does not seem very likely on the basis of the inherent slowness of these disproportionation reactions. Another reason could be related to the difficulty of protonation of the oxo bridge in the reduced form of **1** which would impede the disproportionation reaction or simply the breakage of the bridge. It is not clear, then, why the protonation of the oxo bridge would occur for **2** and not for **1**, except if one assumes that the extra pyridine groups in **1** compete efficiently for protons with the oxo group. It will certainly be valuable to understand the reason of the kinetic stability of the mixed-valent form of **1**. Whatever the reason be, the observation of the mixed-valent form allowed us to detect an equilibrium implying the chloride ligand and to evaluate the corresponding thermodynamic and kinetic data.

Acknowledgment. We thank the Laboratoire d'Electrochimie Moléculaire, URA CNRS 438, Université Paris VII, for the use of their high-scan rate cyclic voltammetry equipment.

Supporting Information Available: Listings of complete atomic coordinates and *U* values, bond distances and angles, anisotropic displacement parameters, crystal parameters, and hydrogen atom coordinates for **1** and **2** and an ORTEP view of the cation of **1** (14 pages). Ordering information is given on any current masthead page.

IC951084T

(30) Other iron complexes with the ligand bispicMe_2en have been studied by: Arulsamy, N.; Goodson, P. A.; Hodgson, D. J.; Glerup, J.; Michelsen, K. *Inorg. Chim. Acta* **1994**, *216*, 21−29. Hazell, R.; Jensen, K. B.; McKenzie, C. J.; Toftlund, H. *J. Chem. Soc. Dalton Trans.* **1995**, 707. In the latter, the complex [(bispicMe_2en)ClFeOFeCl(bispicMe_2en)]$(ClO_4)_2 \cdot 0.5H_2O$ has been described.

(31) An analogous complex has been described in ref 13.